Manganese and Iron at the Redox Interfaces in the Black Sea, the Baltic Sea, and the Oslo Fjord

S. Pakhomova and E.V. Yakushev

Abstract The joint analysis of the data of manganese and iron species distributions (dissolved Mn, dissolved bound Mn, dissolved Fe(II) and Fe(III), particulate Fe and Mn) obtained in the Black Sea, the Baltic Sea, and the Oslo Fjord allowed to reveal the common features that testify the similarity of the mechanism of the redox layer biogeochemical structure formation in these regions. Our investigations demonstrated that Mn bound in stable complexes with hypothetically organic matter or pyrophosphate is observed in the redox zones in significant concentrations (up to 2 μM), and is likely presented by Mn(III), an intermediate product of Mn(II) oxidation and Mn(IV) reduction. This bound Mn(III) can explain phosphate distribution in redox interfaces – formation of so-called phosphate dipole with a minimum above the sulfidic boundary and a maximum just below, and with a steep increase in the concentrations between these two. This dipole structure serves as a geochemical barrier that decreases the upward flux of phosphate from the anoxic layer. On the base of the recent data obtained in the 100th cruise of RV "Professor Shtokman" (March to April, 2009), it was found that the bound Mn could exist in two forms – colloidal (0.02–0.40 μm) and truly dissolved (<0.02 μm) that perhaps result from complexing with different types of ligands. The flushing events, river input, sporadically increased mixing, and anoxygenic photosynthesis affect the distributions of the redox zone parameters. Response time for changes in the microbial processes involved in reduction and/or reoxidation of Mn and Fe lags

S. Pakhomova (✉)
P.P.Shirshov Institute of Oceanology of the Russian Academy of Sciences (SIO RAS), 36, Nakhimovskiy Pr., 109017 Moscow, Russia
e-mail: s-pakhomova@yandex.ru

E.V. Yakushev
P.P.Shirshov Institute of Oceanology of the Russian Academy of Sciences (SIO RAS), 36, Nakhimovskiy Pr., 109017 Moscow, Russia
and
Norwegian Institute for Water Researches (NIVA), Gaustadalléen 21, 0349 Oslo, Norway

behind that for oxygen injection into water. Concentrations of redox-sensitive species of Mn and Fe should thus be useful as a tracer to inter prior hypoxic/anoxic conditions not apparent from oxygen levels at the time of sampling. Modeling results showed that the manganese cycle [formation of sinking down Mn(IV) and presence of dissolved Mn(III)] is the main reason of oxygen and hydrogen sulfide direct contact absence. Modeling allowed to study the role of affecting factors in the formation of the observed distributions.

Keywords Baltic Sea, Black Sea, Iron, Manganese, Oslo fjord, Redox zone

Contents

Abbreviations

B-Chl-e	Bacterial chlorophyll-e
DO	Dissolved oxygen
Fe(II)	Dissolved bivalent iron
Fe(III)	Dissolved trivalent iron
Mn-bou	Dissolved bound trivalent manganese Mn(III)
Mn-diss	Dissolved manganese Mn(II)
Mn-part	Particulate manganese Mn(IV)
NRL	Nepheloid redox layer
OM	Organic matter
SPM	Suspended particulate matter

1 Introduction

The cycles of manganese and iron in the changeable oxic/anoxic conditions are similar. Reduced forms of these compounds are dissolved. They diffuse upward where they oxidize and transfer to oxidized particulate forms that sink down and

reduce in hydrogen sulfide zone. The oxidation–reduction potentials and constants of reaction of oxidation of iron and manganese differ, and these reactions can occur in different amount of oxygen. Due to this, the depth of appearance of particulate manganese is located shallower than of particulate iron [1]. Bacteria have been shown to oxidize manganese [2], whereas iron oxidation is possible without bacteria but can be carried out with bacteria [3]. Reduced iron can be oxidized by particulate manganese, forming complex compounds [4].

According to the recent estimates, the biogeochemical structure of the water column redox layer is characterized by an absence of overlap between dissolved oxygen and hydrogen sulfide and presence of a suboxic zone, where both oxygen and hydrogen sulfide are below detection limits [5]. Oxygen disappears at a depth where the onset of ammonia and dissolved manganese is observed, while hydrogen sulfide appears in the Black Sea water column approximately 5–10 m deeper. In this layer, reduced and oxidized forms of several elements (N, S, C, Mn, Fe) can be observed, which reflects the complexity of processes occurring in this zone.

The role of cycles of different elements in the formation and support of the redox layer balance and biogeochemical structure is still not clear, particularly the reasons for the phenomenon of the suboxic zone existence [5]. One of the possible explanations can be connected with the manganese cycle [6]. The general scheme invoked to explain this phenomenon is the diffusion of reduced, dissolved Mn(II) up from the anoxic zone into the suboxic zone where it is oxidized biologically to solid phase Mn(IV) oxides. This promotes a sinking flux of Mn oxides that is reduced chemically by sulfide.

Recently Mn(III) was observed in the marine environment [7], an important intermediate product of the Mn cycle that could be formed both at Mn(II) oxidation [8, 9] and at Mn(IV) reduction [10, 11]. This dissolved oxidized Mn(III) could explain distribution of other elements in redox interfaces such as phosphate because of possibility forming P-containing complexes [9]. This oxidized and dissolved phase has only been revealed in recent years, and it became necessary to investigate its distributions in the natural systems to estimate its role on the redox zone structure formations. This form was not represented in suboxic zone models that seek to describe the flow of primary nutrients such as nitrogen, phosphate, and carbon as well as heavy metals through the oxic/anoxic boundary.

Iron concentrations in the water column are much smaller than the Mn ones, but nevertheless iron can probably also affect the structure of the redox zones; for example, there was proposed recently a mechanism of the coupling of the Mn and Fe cycling in the particles formed at the redox boundaries [12]. But there are still not enough accurate data on the iron forms distributions at the redox interface.

We suppose that the comparison of the biogeochemical structures of the redox interfaces from the different regions can give unique information necessary for understanding the processes occurring there. A numerical model can be a useful tool for analyzing these processes. This chapter is aimed for summarizing a new data received during the last years in the field of Mn and Fe biogeochemical cycling at the water column redox interfaces.

2 Methods

2.1 Study Site

Distributions of chemical parameters in the redox zone were studied in the north-eastern and the central Black Sea, the Baltic Sea (Gotland and Landsort Deeps), and the Oslo Fjord on board of RV "Akvanavt," "Ashamba," RV "Professor Shtokman"; RV "Professor Albrecht Penck"; RV "Poseidon" and RV "Uttern," respectively, during July 2004 to August 2009. The geographic locations of the study areas are given in Fig. 1.

The Black Sea redox interface is characterized by the most stable biogeochemical structure among comparable interfaces (i.e., Cariaco trench, Baltic Sea's anoxic deeps). In the whole Black Sea area, with an exception of the Bosphorus region, the chemical features are connected with the density structure and the vertical fluxes of main reductants and oxidants seem to be in balance, while the horizontal exchange is negligible.

The redox zones of the Gotland and Landsort Deeps of the Baltic Sea (240 and 450 m deep, respectively) are subjected to the influence of intrusions virtually throughout the whole year and observed features are usually complex due to a lack of equilibrium.
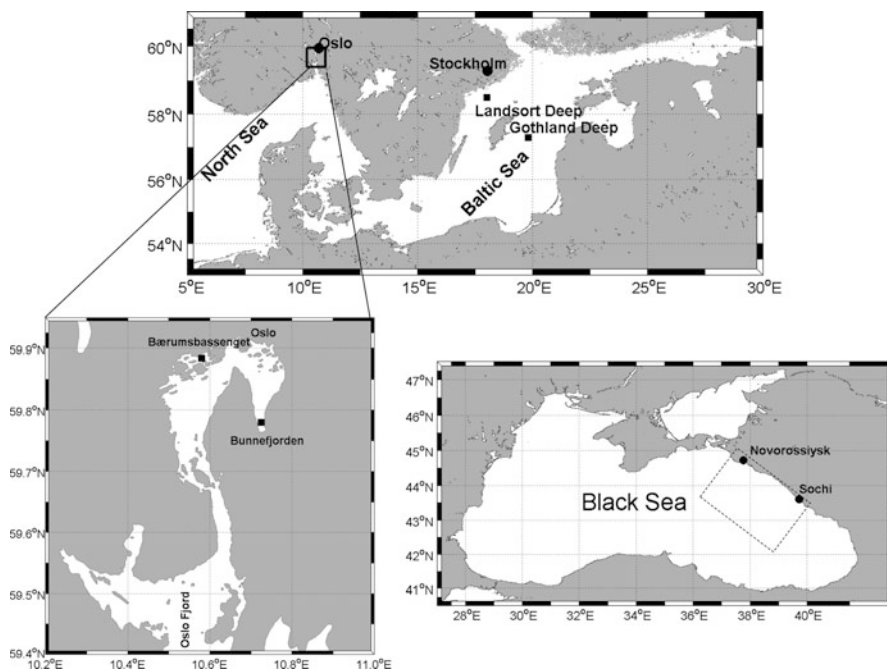

Fig. 1 Sampling locations in the Baltic Sea (**a**), the Oslo Fjord (**b**) and the Black Sea (**c**)

The Baerumsbassenget is a small part of the Oslo Fjord with an approximate area of 5 km^2 and a maximum depth of 31 m. It is separated from the main fjord through a series of islands with a maximum sill depth of 15 m. The inflow into the Baerumsbassenget, the Sandvika River, is responsible for the formation of its permanent meromictic structure with redox interface positioned in the euphotic zone (15–20 m). Bunnefjorden is a 160-m deep anoxic basin, with flushing ones per several years, redox interface at about 90 m.

2.2 Sampling

Water samples for chemical measurements were collected using a Rosette equipped with 5-L Niskin bottles and using pump systems. The used pump system was based on an onboard 12 V peristaltic pumps, with a 11-mm hose attached to the CTD probe. The time of the hose flushing was about 10 min for 170-m hose used in the Black Sea and about 1 min for 20-m hose used in the Oslo Fjord. These pump systems allowed to sample water protected from contamination with the atmospheric oxygen that is essentially for the suboxic systems studies. In our studies, we used the AANDERAA Optode 3835 sensor to measure oxygen concentrations in the hose during the sampling. In the Baltic Sea cruise, the Institute for the Baltic Sea Research's Warnemuende pump system with a pump established at the CTD probe [13] was used.

Sampling in the suboxic zone was performed at 2–3 m intervals in the Black and Baltic Seas and at 0.5–1 m intervals in the Oslo Fjord, aiming to obtain detailed data of the distribution of chemical parameters.

2.3 Chemical Measurements

Dissolved oxygen (Winkler), hydrogen sulfide, phosphate, polyphosphate, nitrate, nitrite, ammonia, and hydrogen sulfide were measured using the standard methods [14–18].

Water samples for dissolved metal analysis were filtered through 0.4-μm Nuclepore filters immediately after sampling. Dissolved manganese and dissolved iron (II), iron (III) concentrations were determined spectrophotometrically using the formaldoxime and ferrozine procedures, respectively [15, 19]. Dissolved organic matter was decomposed using UV irradiation with an addition of hydrogen peroxide (50 μL of 30% H_2O_2 per 20 mL of sample) at pH 2 during 1 h. An 80-W high-pressure Hg lamp was used as a source of UV radiation. Then total dissolvable metals concentration was determined spectrophotometrically. We called the difference between total dissolvable and dissolved metal bound manganese (Mn-bou) and iron (Fe-bou). Precision of dissolved metal analysis was typically 3%. Detection limits were 20 and 100 nM for iron and manganese, respectively.

Water samples for particulate iron and particulate manganese analyses were collected in 2-L plastic bottles. Filtration of water was undertaken no later than several hours after sampling using a Millipore filtration system and thoroughly washed and weighed 0.4 μm filters. Analyses of particulate metals were carried out by AAS following wet acid dissolution of the filters. Particulate Mn concentrations were also estimated as a difference between the spectrophotometric measurements of dissolved manganese in the filtered (0.4 μm) and unfiltered samples [Mn-part(ded)].

2.4 Modeling

For the analysis of the distribution of parameters, we used a coupled hydrophysical-biogeochemical one-dimensional O–N–S–P–Mn–Fe model based on RedOx Layer Model (ROLM) [20] and one-dimensional General Ocean Turbulent Model (GOTM) [21]. Processes of organic matter (OM) formation and decay, the reduction and oxidation of species of nitrogen, sulfur, manganese, iron, as well as transformation of phosphorus species are parameterized in ROLM. The model equations and parameters used and a detailed description are presented in [22]. ROLM was coupled with GOTM, and we used GOTM software to perform numerical calculations.

3 Results

3.1 Manganese

The data on dissolved inorganic manganese, Mn(II), obtained in *the Black Sea* (Figs. 2–5), are in agreement with the previous studies [1, 23, 24]. The characteristic features of the Mn(II) distribution are: (1) a low (nanomolar) content in the surface waters; (2) an intensive increase at the boundary of the sulfidic zone reaching maximum values of 8–10 μM in the first tens meters of the sulfidic zone; (3) a decrease to 4–5 μM and a relative stability of concentrations in the deep water.

The lack of Mn(II) in the upper layer can be explained by a formation under the oxic conditions of insoluble oxides [25, 26] that precipitate and therefore remove Mn from the upper layer.

In the suboxic zone and in the upper part of the anoxic zone, the concentrations of Mn(II) increase and reach its maximum values about 30–40 m below the sulfide boundary (Fig. 2). The vertical gradient of Mn(II) is maximal in the vicinity of the sulfide boundary (up to 0.55 μM/m). It decreases in the anoxic zone, while the concentration of dissolved manganese reaches its maximum (8–10 μM). Below this level, the Mn(II) concentrations decreases and remains in the limits 4–5 μM from ~1,000 m to the bottom [27, 28].

Fig. 2 Vertical distribution of dissolved oxygen (O_2), hydrogen sulfide (H_2S), dissolved Mn (Mn-diss) and dissolved Fe(II) in the central Black Sea, 2009
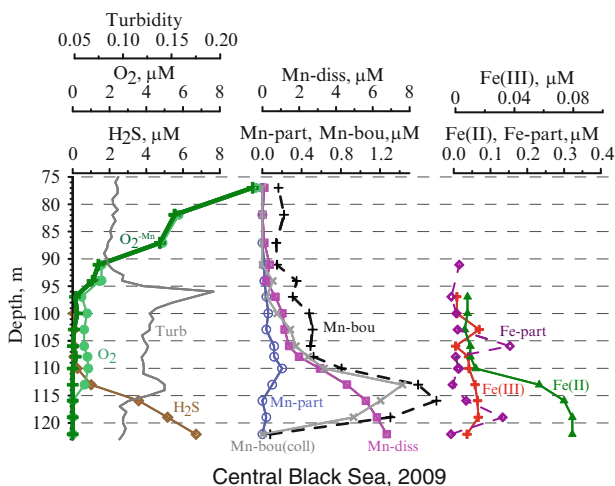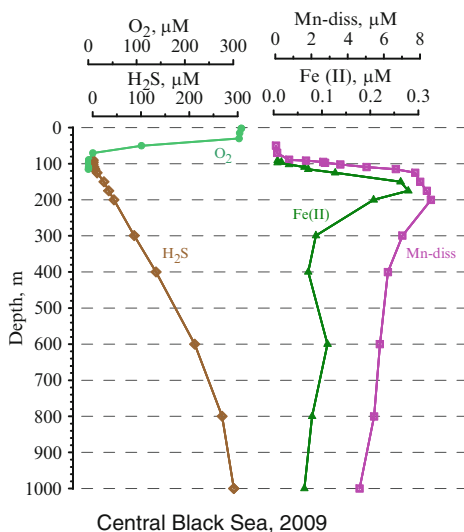

Fig. 3 Vertical distribution of dissolved oxygen measured with Winkler technique (O_2) and after deduction of oxidized Mn forms (O_2^{-Mn}), hydrogen sulfide (H_2S), dissolved Mn (Mn-diss), particulate Mn (Mn-part), bound Mn (Mn-bou), bound Mn in colloidal form (Mn-bou-coll), dissolved Fe(II), dissolved Fe(III), particulate Fe (Fe-part), and turbidity measured with the hydrophysical probe (Turb) in the central Black Sea, 2009

The described structure corresponds to the stable hydrophysical conditions when the upward oxidant and downward reductant fluxes are balanced, and the manganese onset takes place in the layers where the oxygen concentration drops down
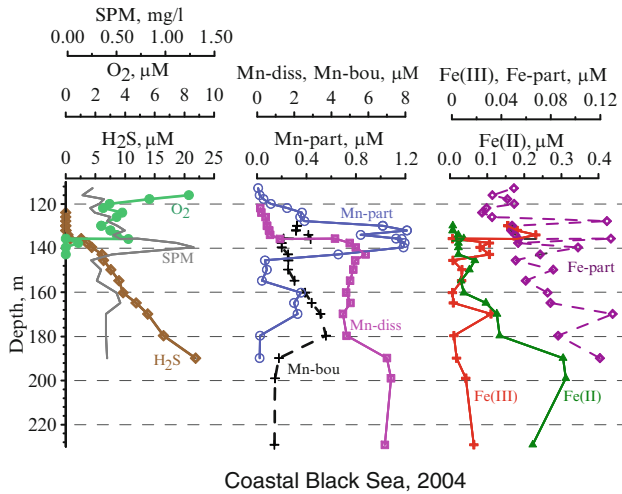
Fig. 4 Vertical distribution of dissolved oxygen (O_2), hydrogen sulfide (H_2S), dissolved Mn (Mn-diss), particulate Mn (Mn-part), bound Mn (Mn-bou), dissolved Fe(II), dissolved Fe(III), particulate Fe (Fe-part), and SPM in the coastal Black Sea, 2004
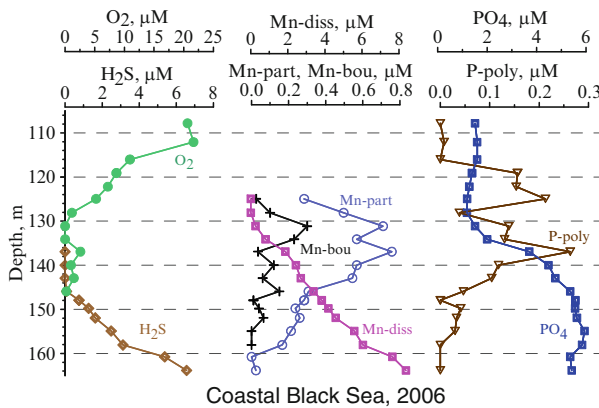

Fig. 5 Vertical distribution of dissolved oxygen (O_2), hydrogen sulfide (H_2S), dissolved Mn (Mn-diss), particulate Mn (Mn-part), bound Mn (Mn-bou), phosphate (PO_4), and polyphosphate (P-poly) in the coastal Black Sea, 2006

below the detection limit [29]. Under certain disturbances, i.e., interaction of the Rim Current and internal waves with the slope, causing vertical displacements of the waters with different densities, or due to the near-slope downwelling [29, 30], oxygen-rich waters can penetrate into sulfide zone. In this case, the stability of the biogeochemical structure disturbs and a messy distribution of elements can be observed. Such changes are registered in the areas affected by the Bosporus current [2, 8, 31] and in the coastal zone near Gelendzhik (Fig. 4) [28, 30].
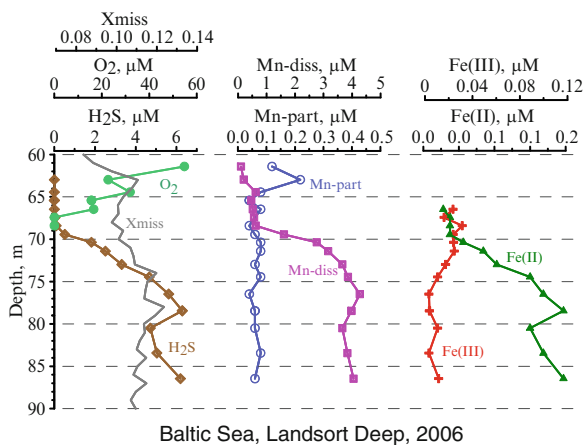
Fig. 6 Vertical distribution of dissolved oxygen (O_2), hydrogen sulfide (H_2S), dissolved Mn (Mn-diss), particulate Mn (Mn-part), dissolved Fe(II), dissolved Fe(III), and transmission measured with the hydrophysical probe (Xmiss) in the Baltic Sea, Landsort Deep, 2006

Fig. 7 Vertical distribution of dissolved oxygen (O_2), hydrogen sulfide (H_2S), dissolved Mn (Mn-diss), particulate Mn (Mn-part), bound Mn (Mn-bou), dissolved Fe(II), dissolved Fe(III), particulate Fe (Fe-part), and transmission measured with the hydrophysical probe (Xmiss) in the Baltic Sea, Landsort Deep, 2006

In *the Landsort Deep, Baltic Sea*, the Mn(II) distribution is close to the Black Sea one with an exception of a formation of well-pronounced maximum closer to the sulfidic boundary (usually the first meters) (Figs. 6 and 7). Mn(II) concentration reaches 4–5 μM and remains in the deeper layers practically constant. The maximal vertical gradient is the same as in the Black Sea.

Fig. 8 Vertical distribution of dissolved oxygen (O_2), hydrogen sulfide (H_2S), dissolved Mn (Mn-diss), particulate Mn (Mn-part), dissolved Fe(II), dissolved Fe(III), and transmission measured with the hydrophysical probe (Xmiss) in the Baltic Sea, Gotland Deep, 2006
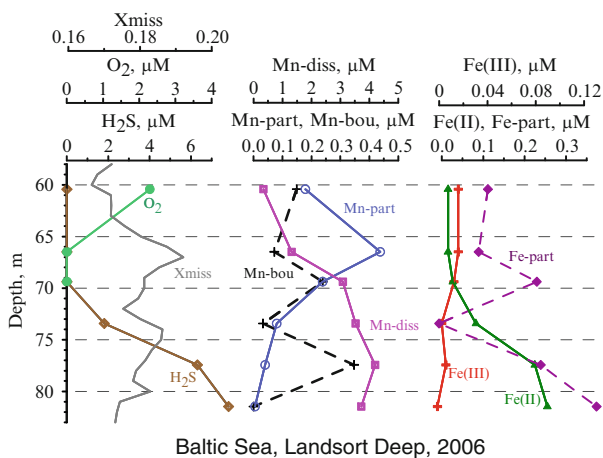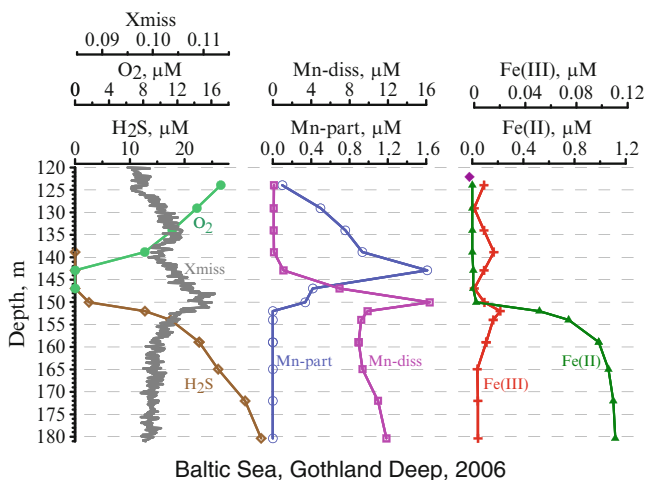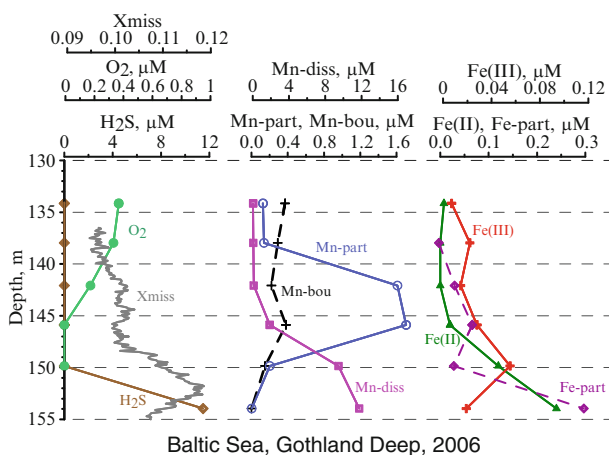

Fig. 9 Vertical distribution of dissolved oxygen (O_2), hydrogen sulfide (H_2S), dissolved Mn (Mn-diss), particulate Mn (Mn-part), bound Mn (Mn-bou), dissolved Fe(II), dissolved Fe(III), particulate Fe (Fe-part), and transmission measured with the hydrophysical probe (Xmiss) in the Baltic Sea, Gotland Deep, 2006

Distribution of dissolved manganese in *the Gotland Deep* is generally characterized by an increase in Mn(II) content with depth in all the sulfidic zone down to the bottom (Figs. 8 and 9). The periodic (ones per several years) oxygenated inflows lead to oxidation and complete vanishing of Mn(II) from the water column. During reestablishment of anoxic conditions, Mn(II) concentrations increase. According to

Table 1 Dissolved manganese near sea bottom concentration in the Gotland Deep

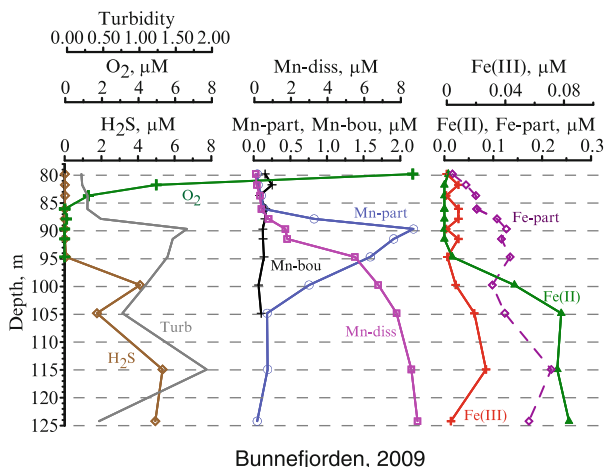| Dissolved Mn, μM	Year	Reference
15–18	1999–2001	Neretin et al. [32]
4	2003	Martens-Habbena, p.c.
30	2005	Our data, RV "Prof. A.Penck"
22	2006	Our data, RV "Prof. A.Penck"
10	2008	Our data, RV "Poseidon"
> 8	2010	Our data, RV "Skagerak"

Fig. 10 Vertical distribution of dissolved oxygen (O_2), hydrogen sulfide (H_2S), dissolved Mn (Mn-diss), particulate Mn (Mn-part), bound Mn (Mn-bou), dissolved Fe(II), dissolved Fe(III), particulate Fe (Fe-part), and turbidity measured with the hydrophysical probe (Turb) in the Oslo Fjord, Bunnefjorden, 2009

the observations, the concentrations in the bottom layer can vary from 4 to 30 μM (Table 1). Frequent oxygen intrusion in the redox zone depth also leads to irregular distribution of Mn(II) there, for example, formation of Mn(II) maximum in the first meters of anoxic zone (Fig. 8). The vertical gradient of Mn(II) is also very changeable and can reach much higher values than in the Black Sea (up to 5.2 μM/m).

In *the Bunnefjorden*, the dissolved manganese reaches its maximal concentration of 8–10 μM in first meters of sulfidic zone, and then its concentrations are practically constant with depth (Fig. 10). Its maximal vertical gradient is about two times higher than in the Black Sea (about 1.1 μM/m).

Dissolved manganese distribution in *the Baerumsbassenget* is distinguished by high variability and has nonuniform character (Figs. 11 and 12). Even manganese concentration is not so high, about 4.5 μM, and the vertical gradient is maximal for the studied regions (5.5 μM/m). The specific feature of manganese distribution in Baerumsbassenget is that the onset of dissolved manganese is observed in more oxic conditions than in other regions, at oxygen concentration about 18 μM.
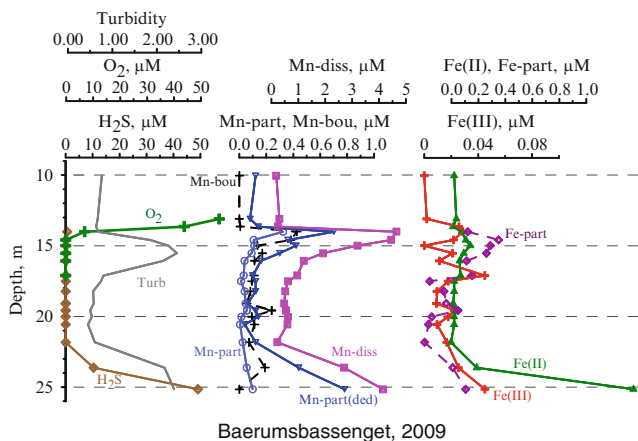
Fig. 11 Vertical distribution of dissolved oxygen (O_2), hydrogen sulfide (H_2S), dissolved Mn (Mn-diss), particulate Mn (Mn-part), particulate Mn determined by deduction of content of Mn in unfiltered sample relative to filtered through 0.4 μm Nuclepore filter immediately after sampling [Mn-part(ded)], bound Mn (Mn-bou), dissolved Fe(II), dissolved Fe(III), particulate Fe (Fe-part), and turbidity measured with the hydrophysical probe (Turb) in the Oslo Fjord, Baerumsbassenget, 2009
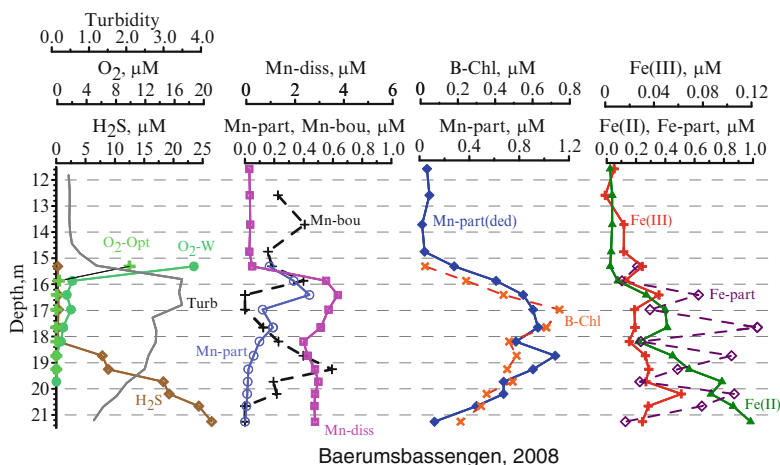
Fig. 12 Vertical distribution of dissolved oxygen measured with Winkler technique (O_2-W) and with Optode (O_2-Opt), hydrogen sulfide (H_2S), dissolved Mn (Mn-diss), particulate Mn (Mn-part), particulate Mn determined by deduction of content of Mn in unfiltered sample relative to filtered through 0.4 μm Nuclepore filter immediately after sampling [Mn-part(ded)], bound Mn (Mn-bou), dissolved Fe(II), dissolved Fe(III) and particulate Fe (Fe-part), turbidity measured with the hydrophysical probe (Turb), and bacteria-Chl-e (B-Chl), in the Oslo Fjord, Baerumsbassenget, 2008

The distribution of the particulate manganese, Mn(IV), in all the regions is characterized by a layer of increased concentration in suboxic zone with a maximum at the hydrogen sulfide boundary (Figs. 3–5, 7, and 9–12). As a rule,

an increase of the concentrations in the oxic zone is enough steep while a decrease in the hydrosulfide zone is more gradual. At the studied regions, the maximum concentration of particulate manganese amounted to 0.2–2.1 μM. The lower content was found in the central Black Sea, and the highest in the coastal Black Sea and the Bunnefjorden.

Dissolved bound manganese, Mn(III), may have several maxima of concentrations located between the particulate manganese and dissolved manganese maxima or can coincide with the Mn(IV) maximum. The concentration of Mn(III) in its maxima amounts in the Black Sea to 0.1–2 μM. In other regions, its concentration does not exceed 0.75 μM (0.5 μM in average). In the Black Sea, bound manganese exists both in colloidal form (0.02–0.40 μm) and truly dissolved (<0.02 μm). Colloidal form could amount up to 90% of bound manganese (Fig. 3).

It is necessary to note that the layers of maxima of both Mn(III) and Mn(IV) are very narrow compared with the possible sampling resolution; therefore the real maximum concentrations and the vertical gradients values can be higher than we can measure.

3.2 Iron

The distribution of dissolved Fe(II) in *the Black Sea* is similar to the manganese one (Figs. 2–4). It is characterized by an increase in the redox zone and the formation of an intermediate maximum within the limits of the dissolved manganese maximum. However, a drastic decrease of the iron (II) concentration takes place deeper as the result of the formation of insoluble iron sulfides.

Under the oxic conditions, Fe(II) rapidly oxidizes to transform into iron (III) represented under these conditions by oxides and hydroxides of low solubility. An increase in the dissolved Fe(II) concentrations occurs at more reduced condition than for dissolved Mn(II) and starts at the sulfidic boundary with a vertical gradient increasing toward the Fe(II) maximum. This maximum of Fe(II) (0.25–0.3 μM on average) is reached at the same depth as the dissolved manganese one. In the deeper layers, Fe(II) decreases to 0.05–0.07 μM, which is controlled by the iron sulfide solubility.

The distribution of Fe(II), as that of Mn(II), is affected by the intrusions of oxic water, which causes its concentration decrease resulting from oxidation.

In *the Landsort Deep* and the *Bunnefjorden*, the distribution of dissolved Fe(II) is quite similar to the Black Sea both by the position of its onset and by the concentration (Figs. 6, 7, and 10). The difference in these regions is that the concentration of Fe(II) does not decrease with depth in sulfidic zone and is practically constant there (0.3 μM) toward the bottom.

Distributions of dissolved Fe(II) for *the Gotland Deep* and the *Baerumsbassenget* differ from those in the Landsort deep and the Black Sea. In most cases, Fe(II) concentration increases toward the bottom and reach up to 1.5 μM in both regions (Figs. 8, 9, 11, and 12). In the Baerumsbassenget, an onset of Fe(II) is located not at

the sulfidic boundary as in other regions but at more oxidized condition at the depth where oxygen goes down below the detection limit.

The distribution of dissolved Fe(III) at all the studied regions is characterized by two maxima of 0.03–0.1 μM. One must note that all the peaks of the dissolved Fe(III) are situated either at the same depths as those of the particulate iron or just below them. The first maximum of Fe(III) coincides with the maxima of dissolved inorganic phosphorus and of particulate manganese. The second maximum of Fe(III) either coincides or is situated a little above the maximum of dissolved Fe(II).

The distribution of particulate iron is characterized by more nonuniformity than that of the particulate manganese, and at most of the stations, the maximum of the particulate iron coincides with that of the particulate manganese. The concentrations of particulate iron in the redox zone of the *Black Sea* amount to 0.04–0.3 μM, excluding the stations affected by the riverine runoff, at which the content of particulate iron may be as high as 2 μM. In the *Gotland*, *Landsort Deeps*, and *Bunnefjorden*, concentration of particulate iron reaches 0.2–0.5 μM, and in the *Baerumsbassenget* it reaches 0.85 μM.

In case of large concentrations, particulate iron may considerably affect the value of turbidity.

4 Discussion

The specific features of the hydrochemical structure observed in the studied objects are summarized in Table 2.

The thickness of the suboxic zone is the largest in the central Black Sea and in the Bunnefjorden. Suboxic zone can be absent in case of such factors as oxygen intrusions, river input, and currents. This was observed in coastal Black Sea, Baltic Deeps, and Baerumsbassenget.

Distribution of dissolved Mn(II) and bound Mn is quite different in the studied regions, while particulate manganese behavior is most similar.

The particulate manganese maximum often coincides with an increased turbidity and a so-called nepheloid redox layer (NRL) can be distinguished there [33]. Besides Mn(IV), a zero-valent sulfur [34], detritus, and bacteria can contribute to a decrease of transparency there. NRL is a usual feature of the Black Sea [28]. In the fjords, NRL usually coincides with maximum of particulate manganese. Only in the Baltic Sea, NRL is located just above the maximum of particulate manganese. Suspended particulate matter (SPM) in the Baerumsbassenget can include together with the manganese oxide, the higher amounts of organic matter and photosynthetic bacteria and has very intensive deep-brown color. Content of SPM in NRL is maximal in Baerumsbassenget (2.5–3.6 mg/l). In other regions it does not exceed 1 mg/l. But manganese content in NRL is minimal in Baerumsbassenget (1.3–1.8%). In the Black Sea its amount is varied from 5% to 15%, in the Bunnefjorden and Gotland Deep is maximal – about 25%.

Table 2 Characteristics of redox zones and Mn, Fe distributions in the Black Sea, the Baltic Sea and Oslo Fjord

Main features	Black Sea		Baltic Sea		Oslo Fjord	
	Center	Periphery	Gotland deep	Landsort deep	Bunnefjorden	Baerumsbassenget
	Stable hydrophysical structure	Enhanced mixing due to RIM current	Oxygen intrusions into suboxic zone	Oxygen intrusions into suboxic zone	Flushing ones per several years	Anoxygenic photosynthesis and river inflow
Depth, m max/redox interface	2,100/70–90	500/140–180	240/115–135	450/60–85	160/80–90	31/16–23
Thickness of suboxic zone, m	10–17	0–12	0–10	0–3	14	1–6
SPMmax, mg/l	0.16–1	1.2–2.4	0.43	0.65	0.5–0.66	2.5–3.6
c(Mn-diss)max, μM	8–10	7–9	16–20	4–4.8	8–10	4–4.6
Grad(Mn-diss) max, $\mu M/m$	0.55	0.4	5.2	0.7	1.1	5.5
c(Mn-part)max, μM	0.2–1	1–2	0.5–1.6	0.3–1.5	1.3–2.1	0.7–1
Mn-part, % in SPM	5.5	15	25	2–4	24	1.3–1.8
c(Mn-bou)max, μM	1.8	0.5	0.75	0.4	0.25	0.4–0.6
c(Fe(II))max, μM	0.34	0.45	1–1.5	0.32	0.33	0.4–1.4
c(Fe(III)-diss) max, μM	0.08	0.05	0.03	0.05	0.03	0.04
c(Fe-part)max, μM	0.15–0.29	0.22–0.48	0.36	0.54	0.18–0.22	0.60–0.85
Grad(Fe(II))max, nM/m	5–10	5	30–600	3–25	19	500

A shallow position of the redox interface at Baerumsbassenget can lead to intensive anoxygenic photosynthesis. The whole cell absorption spectra of the samples show a characteristic absorption peak at 715 nm, indicating the presence of bacterial chlorophyll-e (B-Chl-e) and the photosynthetic bacteria type *Chlorobium* sp. [35]. The vertical distribution of the B-Chl-e in the Baerumsbassenget was characterized by a maximum at 17 m, in the middle of the suboxic zone between the onsets of H_2S and O_2 [36]. The B-Chl-e concentrations decrease rapidly until the appearance of H_2S where this decreases slowed down. A similar structure was observed previously at Framvaren Fjord [37]. The B-Chl-e maximum did not correspond to any minimum in the phosphate curve; however, a strong relationship between the vertical distribution of B-Chl-e and SPM (Fig. 12) was shown.

The content of particulate Mn is a subject to seasonal variability [28, 38, 39]. In the Black Sea, particulate Mn concentrations were approximately 0.35 μM in summer and more than 2 μM in winter–spring, and its portion in SPM varied from 6–12% in summer to 35% in winter [28]. This is due to an increase in organic matter content in SPM during the summer and more intensive vertical mixing in the winter. Pohl et al. [39] showed that in the Baltic Sea (Gotland Deep) the seasonal variability of particulate Mn content in SPM (1–5.5%) occurred, with an increase in winter and a decrease in summer, in addition to a high interannual variability, connected to the Baltic Sea oxygenated flushing events. The data received during 2008 correspond to summer values in the Black Sea, significantly greater than values observed in Landsort Deep during 2006 (0.15–0.4 μM of Mn-part, 2% of SPM, [40]). The latter can be linked with the oxygenated intrusions taking place in Landsort Deep before and during the studies.

Particulate Mn variability in the fjord systems could be higher than in the Baltic Sea due to a larger number of the affecting processes (i.e., river input, tides, storm weather, anoxygenic photosynthesis, etc.). The redox zones in the fjords have more "reduced" character. Suspended Mn practically disappeared from the samples, being measured next day. This never was observed for the Black Sea or Baltic Sea.

Our data demonstrate the presence of the dissolved bound Mn(III) in the vicinity of the redox interface at all the studied redox interfaces. The question is what oxidation state of manganese forms complexes and what type of ligands (organic matter?) are involved in. It is known that stable complexes with OM are not typical for the bivalent manganese. Tebo et al. [8] demonstrated the existence of Mn(III) in complexes with high-stability constant (siderophores, logK = 47.5). Trouwborst et al. [7] studied the distribution of Mn(III) in the southwestern Black Sea water in the RV "Knorr" Black Sea cruise 173–7. According to their data, Mn(III) forms a layer with increased content between the particulate Mn maximum and dissolved Mn(II) maximum. As noted above, our data on the bound Mn correspond well with the values and position of the maximum layer; thus we can assume that this bound Mn is Mn(III) complexes [28].

Mn(III) is an intermediate product of Mn(II) oxidation, and it is in unstable form that has to be complexed to exist in marine conditions. Reduction of Mn(IV) to Mn(II) with hydrogen sulfide can also be provided through an intermediate stage of Mn(III) [10, 11] leading to the additional increase of the Mn(III) pool. Many factors

could influence on Mn(III) presence and its content in the redox zone, i.e., the rate of Mn(II) oxidation and Mn(IV) reduction, presence of Mn-oxidizing bacteria, complexing agents for binging Mn(III) with different stability of formed complexes, the rate of vertical diffusion, etc. In the studied regions, the most favorable conditions for existing of the bound Mn(III) are in the Black Sea, where this form of Mn was found at all the studied station with concentration up to 2 μM. In the Baltic Deeps, the presence of bound Mn(III) in the redox zone is not a usual feature.

The occurrence of trivalent manganese in the redox zone of the Black Sea is of great importance.

First, this is one more oxidant that helps to explain the phenomenon of the suboxic zone and an absence of a layer of coexistence of hydrogen sulfide and oxygen. Dissolved oxygen is measured by Winkler method with adding of manganese compounds. Oxidized manganese forms [particulate Mn(IV) and dissolved Mn(III)] presented in sea water above the hydrogen sulfide zone overstate the results of oxygen determination. For example in the 100th cruise of RV "Professor Shtokman," a total concentration of particulate and bound Mn at the sulfidic boundary was to 0.2–0.5 μM with maximum 1.5 μM. After deduction of these values from dissolved oxygen results obtained by the Winkler titration, a 10-m suboxic layer was distinguished where both oxygen and hydrogen sulfide were absent (Fig. 3) [41]. The presence of this layer conforms to modern theoretical conceptions and experimental investigations (e.g., by measurements with oxygen Optode, Fig. 12).

Second, the properties of the trivalent manganese are similar to those of trivalent iron. For example, these compounds form identical complexes with organic matter of seawater [8, 42], which causes concurrent reactions between them. This is of importance for the distribution and biological availability of dissolved iron.

Third, the presence of large amounts of trivalent manganese in the redox zone may affect the distribution of other elements capable of forming compounds with manganese (e.g., phosphorus). Manganese (III)–pyrophosphate complexes are characterized by the ratio Mn/P = 0.52 for $Mn(HP_2O_7)_2^{3-}$, or Mn/P = 0.17 for $Mn(H_2P_2O_7)_3^{3-}$ [9]. As we think, the possible formation of Mn(III) complexes with pyrophosphates might explain the structure observed for the distribution of phosphates. The upper phosphate minimum is located at the depth where Mn(II) disappears due to the oxidation by oxygen, and the lower minimum of phosphates is located a little below the hydrosulfide interface. On the base of our data received in the autumn 2006 near Gelendzhik (Fig. 5), a polyphosphates maximum can be distinguished between the upper minimum and lower maximum of phosphates, with the location depth conforming to the maximum of the Mn-containing dissolved complexes.

A correlation between the Mn-bou and P-poly concentrations was revealed in the redox zone in the Black Sea and the Landsort Deep with the ratios 1.25 and 0.53, respectively [36]. Virtually no correlation between the Mn-bou and P-poly was found in the Oslo Fjord. It can be explained by the fact that in the Baerumsbassenget the redox interface is located very shallow, and the phosphorus cycle (and P-poly

formation) it affected by the biological activity and the river input. In the Bunnefjorden, the upper phosphate minimum was not pronounced and Mn-bou content in the redox layer was very low (0.1 μM). In addition, Mn(III) can form complexes not only with the phosphorus compounds but also with other organic compounds. The composition of organic matter varies in each basin that leads to the formation of different Mn(III) complexes with a different stability constant able to compete with P-containing ligands. This can therefore result in a variable P/Mn ratio for different regions [36]. On the base of the recent data obtained in the 100th cruise of RV "Professor Shtokman" (March to April, 2009), it was found that the bound Mn could exist in two forms – colloidal (0.02–0.40 μm) and truly dissolved (<0.02 μm) that also testify about Mn(III) complexing with different types of ligands.

A different behavior of dissolved manganese below the hydrogen sulfide boundary was noted for studied regions. In the most of the stations in the Baltic Sea and in the fjords, the concentration of dissolved manganese practically does not change with depth in anoxic zone. In the Black Sea, maximum of dissolved Mn is observed in the first tens of meters of sulfidic zone. After that its concentration decreases to about 4 μM and remains constant till the bottom. The mechanism of this maximum formation is not clear as well why it does not exist in other regions. In general, the manganese transformation in the redox zone is characterized by a cyclic character. Being diffused from the sulfidic zone upward to the oxic zone, dissolved manganese is oxidized to transform into particulate form. These high dense particles precipitate down into the sulfidic zone where it is dissolved. The appearance of colloidal manganese foregoes the beginning of the particulate manganese formation. The bound into complexes Mn(III), as an intermediate of Mn reduction and oxidation, is observed between the maxima of dissolved Mn(II) and particulate Mn(IV). In this case, the dissolution of particulate and colloidal manganese and, probably, the decomposition of manganese complexes enlarge the intermediate maximum of dissolved maximum in the Black Sea. In the other regions, this maximum cannot be formed, because the affecting processes are of different intensity as in the Black Sea, i.e., the rates of Mn oxidation/reduction and dissolution; the rates of Mn(IV) particles sinking; the size of these particles; vertical mixing; formation of solid sulfides and carbonates. According to the model calculations, these solid sulfides and carbonates could exist in the Black Sea anoxic waters [1, 43, 44], but they were never found as in the SPM and in the sediment there. Furthermore, these forms were observed in the Baltic Sea where formation of Mn maximum is not a usual feature. The above-mentioned factors affect also the formation and stability of oxidized Mn(III). We tried to estimate its influence on the redox zone structure using modeling.

In the Baerumsbassenget, it was noted that dissolved Mn concentration started to increase at 18 μM of O_2, 15 m depth, and that manganese reduction in this zone must be an aerobic process. The same situation was observed in the Framvaren Fjord, where the highly organic nature of the water column in fjords suggests that the breakdown of humic acids may be critical in the early redox cycling of manganese [45].

At several stations in all the studied regions, some irregularities in the redox zone manganese species distribution [i.e., secondary maxima of Mn(III, IV), changeable gradient of Mn(II)] were observed, while the distributions of O_2 and H_2S were typical (Fig. 4) (for details, see [28]). Under coastal runoffs, currents, etc., the oxic water may be supplied into the anoxic zone. In this case, the stationary conditions of the system are broken and a nonuniform distribution of elements can occur. It is known that different time periods are needed for different elements to return to a stable equilibrium state. Response time for changes in the microbial processes involved in the reduction and/or reoxidation of Mn lags behind that for oxygen injection into water [46]. Concentrations of redox-sensitive species of Mn should thus be useful as a tracer to inter prior hypoxic/anoxic conditions not apparent from redox conditions at the time of sampling.

The above discussion will also impact upon the iron cycle. Distributions of the iron species depend on redox conditions much stronger than the manganese ones, and it seems that the reactions of iron oxidation/reduction occur very fast. Fe(II) was never observed at oxic conditions in contrast to Mn(II). So, the presence of Fe(II) in the absence of detectable oxygen and hydrogen sulfide could indicate to the reduced condition of the system (Fig. 11).

The iron content within the composition of the NRL suspended matter is as high as 1–5.6% in all the studied regions (about 2% in average). In the Gotland Deep and Bunnefjorden, content of Mn-part in the NRL is much higher than that of Fe-part. In the Landsort Deep, their concentrations are comparable. In the Black Sea, both cases were observed. Only in the Baerumsbassenget, Fe-part content exceeds Mn-part content up to ten times practically in all samples. It could be caused by an intensive iron supply with a river and a release from the sediment settled 10–20 m deeper the redox zone. Difference in dissolved Mn(II) and Fe(II) concentrations is also minimal in this basin among the studied regions.

One can conclude that because of its low content in the redox zones, iron does not play any significant role in the formation of the redox interface structure in studied regions with the exception of Baerumsbassenget.

At several stations in the Black Sea, we tried to measure iron bound in stable complexes. Our data show that iron bound into stable, evidently organic, complexes in the water amounts to 0.1–0.5 μM (not shown, see details in [28]). The distribution of bound iron is characterized by two layers of increased iron content: in the oxygenated intermediate water and just under hydrogen sulfide boundary [28]. The first one could coincide with either the upper maximum of the nitrite or positions just above it, and is related probably to the organic matter, which is revealed by fluorescence. The decomposition of plankton organic matter may cause an increase in nitrate and organic iron forms. The second, deep maximum is usually several times lower than to the shallow one. We may suppose that the high concentrations of dissolved bound iron in the layers of maximum can be related to the terrigenous supply of iron and to the biogeochemical transformation to dissolved complexes of OM in the photic layer and below. As a result, a considerable fraction of iron remains dissolved [42, 47–49]. These organic iron complexes are inert; the logarithm of their stability constants may be as high as 45 [42] and they could exist in the colloidal state

[49]. It seems that due to low concentrations of iron bound into the complexes, this compound does not play any important role in the redox processes.

The data we received confirm the existing theories about the functioning of biogeochemical cycles of Mn and Fe. The reduced forms of these metals are soluble compounds supplied by diffusion from the hydrosulfide zone upward, where they are oxidized to transform into the oxidized particulate forms. These forms, due to their higher density, go downward where they are into dissolved forms. This is superposed by the processes of sulfidization and formation of insoluble iron sulfides. The reduced forms of both iron and manganese interact with oxygen. However, the redox potentials and the rate constants of these reactions are different, and the proper reactions may proceed at different contents of oxygen. Manganese is oxidized under the action of bacteria; iron oxidation is possible without bacteria. The reduced iron may be oxidized by particulate manganese to form complex compounds. The layers of particulate iron formation are located lower and those of manganese are higher, which, in general, conforms to the thermodynamics of these processes. The locations of the layers of the maxima of the dissolved manganese and iron in the upper part of the hydrogen sulfide zone also agree with this sequence.

5   Modeling

The redox-interface chemical structure and the abnormality of the distributions of certain parameters are subject to a number of factors. An effective method of analyzing the roles of these factors is the mathematical modeling. In general, the data obtained on the distribution of the different forms of manganese and iron, their seasonal variability, and their influence on the processes occurring in the redox zone are in agreement with the modeling we performed, which are described in detail in [20, 22, 36].

The modeling studies showed that the formation of tetravalent manganese might considerably affect the distribution of the suspended matter and the formation of the layer of turbidity [6]. The particulate manganese may be a primary oxidant of hydrogen sulfide into elementary sulfur. The intense vertical transfer of detritus grains with the heavy particles of Mn (IV) oxide is a cause of the existence of the zone with no detectable oxygen concentrations (Fig. 13).

This makes possible the processes of anoxic oxidation of reduced compounds, such as methane, reduced iron, and ammonium [20].

The theoretical requirement of the occurrence of seasonal variations of the particulate manganese concentrations was also confirmed by means of the model [20] that treated this phenomenon according to the competition for dissolved oxygen between the organic matter supplied from the upper layers and the reduced compounds supplied from the hydrosulfide zone. This competition results in a fact that the processes of the organic matter mineralization become more intense in the summer; hence, less oxygen is available for the oxidation of the reduced forms of
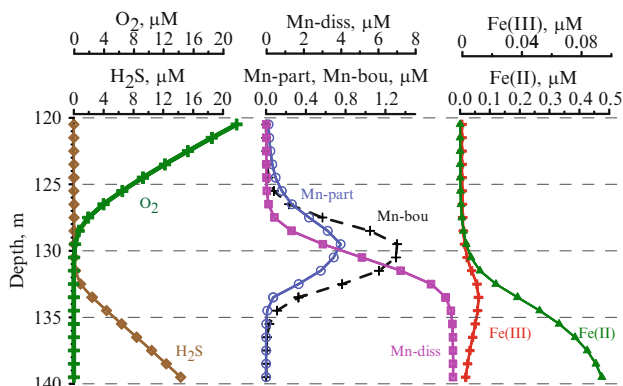
Fig. 13 Vertical distribution of dissolved oxygen (O_2), hydrogen sulfide (H_2S), dissolved Mn (Mn-diss), particulate Mn (Mn-part), bound Mn (Mn-bou), dissolved Fe(II), and dissolved Fe(III) calculated in the model

manganese, iron, and sulfur. At the same time, more oxygen is available for the formation of particulate manganese and iron.

The modeling calculations [20] considering Mn(III) as an independent parameter showed that Mn(III) might oxidize 43% of the sulfides against 50% for Mn(IV). Thus, the total amount of sulfides oxidized into elementary sulfur by oxidized Mn compounds amounts to 93%.

By means of this model, a numerical experiment was performed on the effect of the different processes on the formation of the phosphate distribution profiles. These factors may be (1) chemosynthesis, (2) coprecipitation with metal oxides, and (3) the formation of pyrophosphate complexes with Mn(III). As seen from Fig. 14, at the absence of all three factors listed, the phosphates behave conservatively at the interface area (Fig. 14a). The addition of the chemosynthesis process (Fig. 14b) or of coprecipitation with iron hydroxides (Fig. 14c) causes no pronounced changes. However, the involvement of the process of complexation with Mn(III) allows one to obtain a distribution close to that observed and clearly reproducing the distribution minimum above the hydrosulfide interface and a drastic decrease of the phosphates down to the appearance of hydrogen sulfide (Fig. 14d). According to [9], the Mn:P ratio in the Mn(III)–pyrophosphate complexes may be equal to 0.25 for $Mn(HP_2O_7)_2^{3-}$, or 0.17 for $Mn(H_2P_2O_7)_3^{3-}$. In this model [20], the Mn:P value was 0.66, i.e., even higher by a factor of 2.5–4 than according to [9]. With this ratio, only about 25% of the total Mn(III) should form complexes with pyrophosphates, whereas the remaining fraction may be bound to other ligands. The concentrations of Mn(III) calculated by the model amount to 0.2 μM, which is lower than those usually observed (see above). However, the "phosphate dipole" can be explained even if a part of this Mn(III) forms complexes with phosphorus.

The parameterization of the difference of the rates of the iron and manganese transformation in the model [20] allowed us to reproduce the distribution of the iron
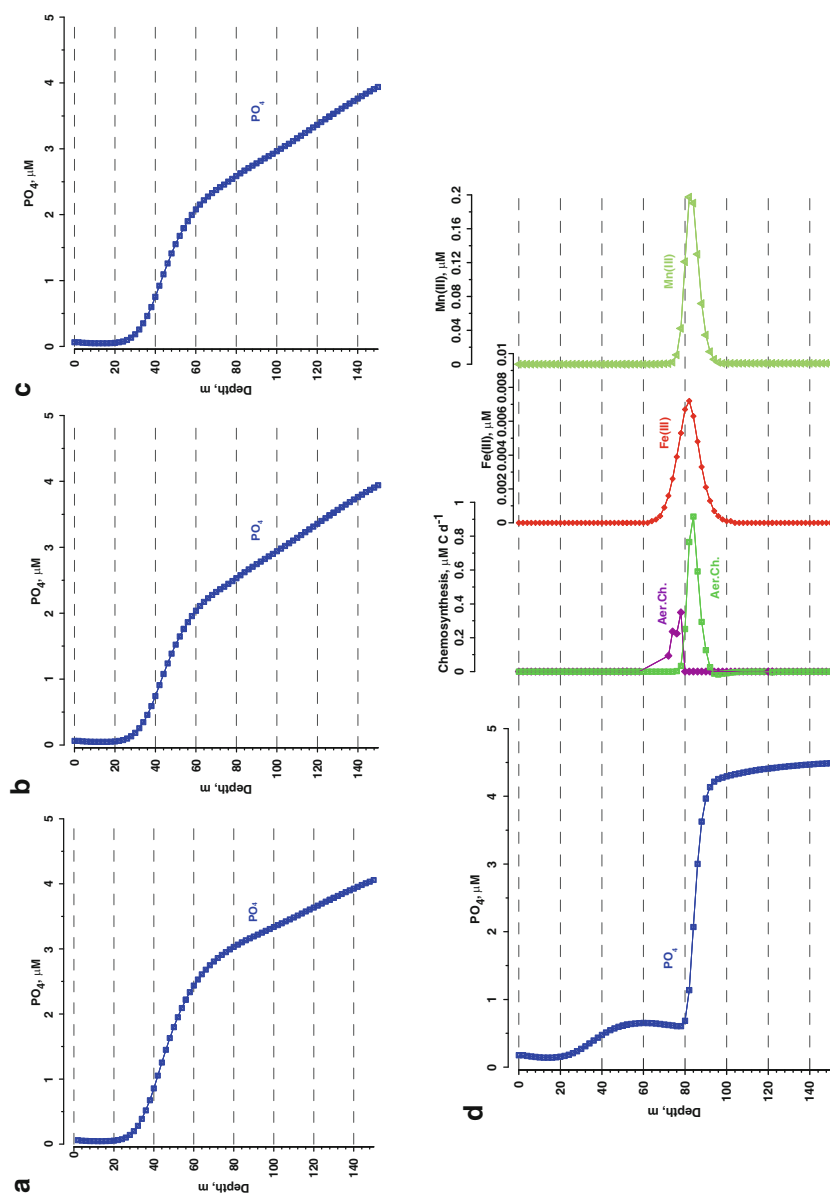
Fig. 14 Model experiments on phosphate minimum formation: (**a**) without influence of Fe(III), chemosynthesis and Mn(III); (**b**) with influence of Fe(III); (**c**) with influence of Fe(III) and chemosynthesis; (**d**) with influence of Fe(III), chemosynthesis and Mn(III), and distributions of chemosynthesis rate, Fe(III), and Mn(III)

forms qualitatively similar to that observed (Fig. 13). The model experiments allow one to conclude that, because of the small concentrations, the role of the iron cycle is insignificant in the formation of the main features of the boundary layer structure between the hydrosulfide and oxic waters.

We used our model to consider the influence of vertical mixing, rate of Mn particles sinking, dissolved Mn content and anoxygenic photosynthesis on the oxidized Mn species, phosphate distributions, and on the suboxic zone wide. Some results of these simulations are presented in Table 3 (in detail, it is described in [36]). One can see that the changes of all studied factors separately could be of great importance for the redox zone structure. In nature, all mentioned factors are not constant and can vary from region to region and from time to time. Their exact combination results in the shape of the distribution of observed parameters.

6   Conclusions

The joint analysis of manganese and iron species distributions (dissolved Mn, dissolved bound Mn, dissolved Fe(II) and Fe(III), particulate Fe and Mn) data obtained in the northeastern Black Sea, the Gotland, and Landsort Deeps of the Baltic Sea and the Oslo Fjord enabled common features to be revealed that demonstrate the similarity of the redox layer formation mechanism in these geographical regions.

Our investigations demonstrate that Mn bound in stable complexes with hypothetical organic matter or pyrophosphate is observed in the redox zones at significant concentrations (up to 2 μM), and is likely present as Mn(III), an intermediate product of the oxidation of Mn(II) and reduction of Mn(IV). This bound Mn plays an important role in the cycle of Mn, and in the cycles of other elements in the redox zone both as oxidizer and complexing agent. It was found that the bound Mn could exist in two forms – colloidal (0.02–0.40 μm) and truly dissolved (<0.02 μm) that perhaps results from complexing with different types of ligands.

Redox interfaces are characterized by the formation of a so-called phosphate dipole with a minimum above the sulfidic boundary and a maximum just below, with a steep increase in concentrations between the two. The hypothesis that P and Mn cycles are interconnected by the formation of complexes between Mn(III) and P-containing ligands can explain the presence of the shallow phosphate minimum above the sulfide interface. The presence of the deep phosphate minimum (below the H_2S boundary) is probably due to the formation of P-containing iron particles [12].

Further studies of the relation between the Mn(III), pyrophosphates, and polyphosphates are of importance to better understand the ecology of seas with anoxic conditions, because the flux of phosphates to the anoxic zone affects the processes of OM production.

Table 3 Simulated by modeling changes in the redox zone structure under different factors. Initial structure parameters: $K_z = 3.5 \times 10^{-5}$ m² s⁻¹, W-Mn(IV) = 7.5 md⁻¹, Mn(II)max = 10 μM, Mn-part≈Mn-bou = 0.8 μM, suboxic zone wide – 3 m

Factors		Suboxic zone wide	Oxidized Mn species	Mn-part/Mn-bou	Example of existence
Vertical mixing	High, $K_z = 3.5 \times 10^{-5}$	Absent, C-layer formed	Increase	>	Black Sea near Bosphorus or RIM current
	Low, $K_z = 1 \times 10^{-6}$	Increase, > 5 m	Decrease	≈<	Central and Coastal Black Sea
Mn particles sinking rate	High, W = 40 md⁻¹	Increase, ≈ 5 m	Decrease	<	Central Black Sea
	Low, W = 0.5 md⁻¹	Present, no changes	Increase	>>	Coastal Black Sea, Gotland Deep, Bunnefjorden
Maximal Mn(II) concentration	High, 30 μM	Increase, >20 m	Increase	≈<	–
	Low, 5 μM	Disappear, O₂ & H₂S depleted in the same level	No changes	≈	Landsort Deep
Anoxygenic photosynthesis		Increase, >20 m	Decrease	≈	Baerumsbassenget

The flushing events, river input, and sporadically increased mixing and anoxygenic photosynthesis play an important role in the formation of redox zones. Response time for changes in the microbial processes involved in reduction and/or reoxidation of Mn and Fe lags behind that for oxygen injection into water. Concentrations of redox-sensitive species of Mn and Fe should thus be useful as a tracer to inter prior hypoxic/anoxic conditions not apparent from oxygen levels at the time of sampling.

Modeling results confirm that exactly manganese cycle [formation of sinking down Mn(IV) and presence of dissolved Mn(III)] is the main reason of oxygen and hydrogen sulfide direct contact absence. Because of the small concentrations, the role of the iron cycle is insignificant in the formation of the main features of the boundary layer structure between the hydrosulfide and oxic waters. The model experiments enabled the role of a number of factors to be assessed. We suggest that in nature all the factors analyzed (amount of Mn, intensity of mixing, sinking rate) are not constant and can vary from region to region and from time to time. Their exact combination results in the shape of the distributions of the observed parameters.

The further studies of the manganese and iron cycling at the changeable redox conditions are necessary to understand the consequences of oxygen depletion development, i.e., effects for transformation of nutrient and hazardous substances.

References

1. Lewis BL, Landing WM (1991) The biochemistry of manganese and iron in the Black Sea. Deep-Sea Res II 38:S773–S803
2. Tebo BM (1991) Manganese(II) oxidation in the suboxic zone of the Black Sea. Deep-Sea Res II 38:S883–S905
3. Canfield DE, Thamdrup B, Kristensen E (2005) Aquatic geomicrobiology. In: Southward AJ, Tyler PA, Young CM, Fuiman LA (eds) Advances in marine biology, 48. Elsevier Academic Press, Amsterdam – Tokio, p 640
4. Dubinin AV (2005) Geochimiya redkozemelnykh elementov v okeane (Geochemistry of the rare earth elements in the ocean). Naukja, Moscow
5. Murray JW, Codispoti LA, Friederich GE (1995) Oxidation–reduction environments. The suboxic zone in the Black Sea. In: Huang CP et al (eds) Aquatic chemistry: interfacial and interspecies processes, ACS advances in chemistry series 244, pp 157–176
6. Yakushev EV, Debolskaya EI (2000) Particulate manganese as a main factor of oxidation of hydrogen sulfide in redox zone of the Black Sea. In: Oceanic fronts and related phenomena. Konstantin Fedorov Memorial Symposium. Pushkin, Saint-Petersburg, Russia. 18–22 May 1998. Proceedings. IOC Workshop Report No. 159. Kluwer Acad. Publ., 2000, pp 592–597
7. Trouwborst RE, Brian GC, Tebo BM, Glazer BT, Luther GW III (2006) Soluble Mn(III) in Suboxic Zones. Science 313:1955–1957
8. Tebo BM, Clement BG, Luther GW III, Trouwborst RE, Webb SM, Bargar JR, Parker DL, Sposito G (2005) The mechanism of bacterial manganese(II) oxidation and its implication for maintenance of the suboxic zone in the Black Sea. In: Program and abstracts of international ocean research conference, Paris, France, p 154, 5–10 June 2005

9. Webb SM, Dick GJ, Bargar JR, Tebo BM (2005) Evidence for the presence of Mn(III) intermediates in the bacterial oxidation of Mn(II). PNAS 102:5558–5563

10. Kostka JE, Luther GW III, Nealson KH (1995) Chemical and biological reduction of Mn(III)-pyrophosphate complexes: potential importance of dissolved Mn(III) as an environmental oxidant. Geochim et Cosmochim Acta 59:885–894

11. Ali K, Ashiq U (2004) Study of the kinetics and activation parameters of reduction of Mn (III) to Mn(II) by SO_3^{2-} ion in $(MnSiW_{11}O_{40}H_2)_5$- heteropoly ion. J Iran Chem Soc 1:122–127

12. Dellwig O, Leipe T, Glockzin M, Marz C, Pollehne F, Schnetger B, Yakushev EV, Brumsack H-J, Böttcher ME (2010) A new particulate Mn-Fe-P-shuttle in the water column of anoxic basins. Geochim Cosmochim Acta. doi:10.1016/j.gca.2010.09.017

13. Krueger S (2004) Operating manual, integrated IOW/MPI PUMP CTD System, IOW, Warnemuende Germany; <Siegfried.Krueger@iowarnemuende.de>

14. Bordovskiy OK, Chernyakova AM (eds) (1992) Modern methods of the ocean hydrochemical investigations. P.P.Shirshov Institute of Oceanology, Moscow, p 200 (in Russian)

15. Grashoff K, Kremling K, Ehrhard M (1999) Methods of seawater analysis, 3rd completely revised and extended edition. WILEY-VCH, Weinheim

16. Hansen HP (1999) Determination of oxygen. In: Grashoff K, Kremling K, Ehrhard M (eds) Methods of seawater analysis 3rd completely revised and extended edition. WILEY-VCH, Weinheim, pp 75–90

17. Hansen HP, Koroleff F (1999) Determination of nutrients. In: Grashoff K et al (eds) Methods of seawater analysis, 3rd completely revised and extended edition. WILEY-VC, Weinheim, p 149–228

18. Koroleff F, Kremling K (1999) Analysis by spectrophotometry. In: Grashoff K, Kremling K, Ehrhard M (eds) Methods of seawater analysis, 3rd completely revised and extended edition. WILEY-VCH, Weinheim, pp 341–344

19. Kononets MYu, Pakhomova SV, Rozanov AG, Proskurnin MA (2002) Determination of soluble iron species in seawater using ferrozine. J Anal Chem 57:704–708

20. Yakushev EV, Pollehne F, Jost G, Umlauf L, Kuznetsov I, Schneider B (2007) Analysis of the water column oxic/anoxic interface in the Black and Baltic seas with a Redox-Layer Model. Mar Chem 107:388–410

21. Burchard H, Bolding K, Kuhn W, Meister A, Neumann T, Umlauf L (2006) Description of flexible and extendable physical-biogeochemical model system for the water column. J Mar Syst 61:180–211

22. Yakushev EV (2011) RedOx layer model. The Handbook of Environmental Chemistry (this volume)

23. Rozanov AG, Volkov II (2002) Manganese in the Black Sea. In: Complex investigations of the northeastern part of the Black Sea. Nauka, Moscow, p 190–200 (in Russian)

24. Yemenicioglu S, Erdogan S, Tugrul S (2006) Distribution of dissolved forms of iron and manganese in the Black Sea. Deep-Sea Res II 53:1842–1855

25. Skopintsev BA (1975) Forming of the modern chemical composition of water in the Black Sea. Hydrometizdat, Leningrad (in Russian)

26. Stumm W, Morgan JJ (1981) Aquatic chemistry. Wiley, New York

27. Yakushev EV, Chasovnikov VK, Murray JW, Pakhomova SV, Podymov OI, Stunzhas PA (2008) Vertical hydrochemical structure of the Black Sea. In: Kostyanoy AG, Kosarev AN (eds) The Black Sea environment, vol 5, The handbook of environmental chemistry. Springer, Berlin, pp 277–307

28. Pakhomova SV, Rozanov AG, Yakushev EV (2009) Dissolved and particulate forms of iron and manganese in the redox zone of the Black Sea. Oceanology 49:773–787

29. Stunzhas PA, Yakushev EV (2006) Fine hydrochemical structure of the redox zone in the Black Sea according to the results of measurements with an open oxygen sensor and with bottle samplers. Oceanology 46:629–641

30. Stunzhas PA (2000) On the structure of the interaction zone of aerobic and anaerobic water in the Black Sea on the base of measurements by membrane-free oxygen sensor. Oceanology 40:503–509
31. Bashturk O, Volkov II, Gekman S, Gungor H, Romanov AS, Yakushev EV (1998) International expedition on R/V Bilim in July 1997 in the Black sea. Oceanology 38:473–476
32. Neretin L, Pohl C, Jost G, Leipe T, Pollehne F (2003) Manganese cycling at the oxic/anoxic interface in the Gotland deep, Baltic Sea. Mar Chem 82:125–143
33. Volkov II, Kontar EA, Lukashev YuF, Neretin LN, Niffeler F, Rozanov AG (1997) The upper boundary of hydrogen sulfide and redox nefeloid layer in water of the Caucasian slope in the Black Sea. Geochemistry 7:540–550
34. Kamyshny A Jr, Yakushev EV, Jost G, Podymov OI (2011) Role of Sulfide Oxidation Intermediates in the Redox Balance of the Oxic-Anoxic Interface of the Gotland Deep, Baltic Sea. The Handbook of Environmental Chemistry. doi:10.1007/698_2010_83
35. Gloe A, Pfennig N, Brockmann H, Trowitzsch W (1975) A new bacteriochlorophyll from brown-colored Chlorobiaceae. Arch Microbiol 102:103–109
36. Yakushev E, Pakhomova S, Sørenson K, Skei J (2009) Importance of the different manganese species in the formation of water column redox zones: observations and modeling. Mar Chem 117:59–70
37. Sørensen K (1988) The distribution and biomass of phytoplankton and phototrophic bacteria in Framvaren, a permanently anoxic fjord in Norway. Mar Chem 23:229–241
38. Ozturk M (1995) Trends of trace metal (Mn, Fe, Co, Ni, Cu, Zn, Cd and Pb) distributions at the oxic-anoxic interface and in sulfidic water of the Drammensfjord. Mar Chem 48:329–342
39. Pohl C, Loffler A, Hennings U (2004) A sediment trap study for trace metals under seasonal aspects in the stratified Baltic Sea (Gotland Basin; 57º19.20'N; 20º03.00'E). Mar Chem 84:143–160
40. Jost G, Clement B, Pakhomova SV, Yakushev EV (2007) Field studies of anoxic conditions in the Baltic Sea during the cruise of R/V Professor Albrecht Penck in July 2006. Oceanology 47:590–593
41. Yakushev EV, Vinogradova EL, Dubinin AV, Kostyleva AV, Pakhomova SV (2011) On the determination of low oxygen concentrations with Winkler technique. Oceanology (in press)
42. Lewis BL, Holt PD, Taylor SW, Wilhelm SW, Trick CG, Butler A, Luther GW III (1995) Voltammetric estimation of iron(III) thermodynamic stability constants for catecholate siderophores isolated from marine bacteria and cyanobacteria. Mar Chem 50:176–188
43. Spenser DW, Brewer PG (1972) Aspect of the distribution and trace element composition of suspended matter in the Black Sea. Geochim Cosmochim Acta 36:71–86
44. Haraldsson C, Westerlund S (1988) Trace metals in the water columns of the Black Sea and Framvaren Fjord. Mar Chem 23:417–424
45. Swarzenski PW, McKee BA, Sørensen K, Todd JF (1999) ^{210}Pb and ^{210}Po, manganese and iron cycling across the O_2/H_2S interface of a permanently anoxic fjord: Framvaren, Norway. Mar Chem 67:199–217
46. Lewis BL, Glazer BT, Montbriand PJ, Luther GW, Nuzzio DB, Deering T, Ma S, Theberge S (2007) Short-term and interannual variability of redox-sensitive chemical parameters in hypoxic/anoxic bottom waters of the Chesapeake Bay. Mar Chem 105:296–308
47. Rue EL, Bruland KW (1995) Complexation of iron(III) by natural organic ligands in the Central North Pacific as determined by a new competitive ligand equilibration/adsorptive cathodic stripping voltammetric method. Mar Chem 50:117–138
48. Van den Berg CMG (1995) Evidence for organic complexation of iron in seawater. Mar Chem 50:139–157
49. Powell RT, Landing WM, Bauer JE (1996) Colloidal trace metals, organic carbon and nitrogen in a southeastern U.S. estuary. Mar Chem 55:165–176